Title: Discrepancies Between Brown Carbon Light-absorption Properties Retrieved from Online and Offline Measurements

Authors: Zezhen Cheng^a, Khairallah Atwi^a, Omar El Hajj^a, Ifeoma Ijeli^a, D. Al Fischer^{b,c}, Geoffrey Smith^b, and Rawad Saleh^{a*}

- Air Quality and Climate Research Laboratory, School of Environmental, Civil, Agricultural, and Mechanical Engineering, University of Georgia, Athens, Georgia, USA
- b Department of Chemistry, University of Georgia, Athens, Georgia, USA
- Now at Department of Chemistry and Physics, Western Carolina University, Cullowhee, North Carolina, USA
- * To whom correspondence should be addressed. rawad@uga.edu | (706) 542-6110,

Abstract:

We compared the imaginary part of the refractive indices (k) of brown carbon (BrC) retrieved from online and solvent-extraction offline light-absorption measurements. BrC with variable light-absorption properties was generated from the controlled combustion of three structurally different fuels: toluene (aromatic), isooctane (branched alkane), and cyclohexane (cyclic alkane). The online retrieval method involved combining real-time measurements of aerosol absorption coefficients (at 422, 532, and 781 nm) and size distributions with Mie calculations. The offline method involved extracting BrC samples with two organic solvents, methanol and dichloromethane, followed by light-absorption measurements of the extracts using a UV-vis spectrophotometer. For the least absorbing BrC, k values of the extracts in both solvents were similar to those of the aerosol. However, for darker BrC, k values of the BrC extracts in dichloromethane were smaller than those of the BrC aerosol, and k values of the BrC extracts in methanol were the smallest, with the discrepancy among the three increasing with increasing BrC darkness. These results indicate that BrC produced in this study was more soluble in dichloromethane than methanol, and the BrC solubility in both solvents decreased with increasing BrC darkness. Finally, k of BrC aerosol and extracts followed the same trend of decreasing wavelength dependence with increasing k as previous data. This further supports the brown-black continuum of light-absorption properties and that the differences observed between k of the BrC aerosol and extracts are due to the inefficiency of solvent extraction and not due to intrinsic differences between the online and offline methods.

1. Introduction

Light-absorbing organic aerosol (OA), or brown carbon (BrC), absorbs incoming solar radiation in the visible and ultra-violet wavelengths (Andreae and Gelencsér 2006; Saleh et al. 2015; Jo et al. 2016; Hammer et al. 2016; Feng, Ramanathan, and Kotamarthi 2013; Wang et al. 2018; Wang et al. 2014). BrC absorption has an important yet uncertain effect on atmospheric radiative balance, with estimates of its global radiative effect ranging over an order of magnitude, between +0.03 W/m² and +0.57 W/m² (Saleh 2020). This large uncertainty is in part a result of persistent gaps in the fundamental understanding of the BrC chemical composition and optical properties. BrC absorption has been linked to various species including polycyclic aromatic hydrocarbons (PAHs) (Saleh et al. 2018; Cheng et al. 2020; Adler et al. 2019), oxygenated and nitrated aromatics (Li, He, Hettiyadura, et al. 2019; Li, He, Schade, et al. 2019; Liu et al. 2016; Liu et al. 2017; Desyaterik et al. 2013; Cheng et al. 2020), nitrogen heterocyclic compounds (Kampf et al. 2016; Marrero-Ortiz et al. 2019), as well as interaction of chromophores with charge transfer complexes (Phillips and Smith 2014, 2015). The diversity in BrC chromophores is manifested as a wide variability in BrC lightabsorption properties, which can be quantified using the wavelength-dependent imaginary part of the refractive index (k) (Chylek et al. 2019). BrC absorption spectra exhibit an increase toward short-visible and UV wavelengths (Laskin, Laskin, and Nizkorodov 2015; Moise, Flores, and Rudich 2015), which can be mathematically represented with a power-law functional dependence on wavelength (i.e., $k(\lambda) \sim \lambda^{-w}$). Based on a compilation of light-absorption data of BrC from various sources reported in the literature, Saleh (2020) proposed an optical classification of BrC based on its k at 550 nm (k_{550}) and w: very weakly absorbing BrC (VW-BrC) (k_{550} =10⁻⁴-10⁻³, w=6-9), weakly absorbing BrC (W-BrC) (k_{550} =10⁻³-10⁻², w=4-7), moderately absorbing BrC (M-BrC) ($k_{550} = 10^{-2} - 10^{-1}$, w = 1.5 - 4), and strongly absorbing BrC (S-BrC) $(k_{550} > 10^{-1}, w = 0.5 - 1.5)$. It is noteworthy that k_{550} of VW-BrC and S-BrC are separated by 3 orders of magnitude and that the more absorptive BrC (larger k_{550}) is characterized by flatter absorption spectra (smaller w). Furthermore, there is a correlation between BrC sources and optical classes, with the more absorptive BrC (M-BrC and S-BrC) mostly associated with high-temperature biomass combustion (Saleh 2020).

In addition to the true variability outlined above, discrepancies between BrC light-absorption properties reported in the literature arise from differences in measurement techniques and the associated biases and uncertainties. Retrieval of *k* and *w* of BrC can be achieved via online aerosol optical measurements coupled with optical (e.g., Mie theory) calculations (Chakrabarty et al. 2010; Saleh et al. 2013; Saleh et al. 2014; Lack et al. 2012) or offline methods involving filter collection and extraction with water or organic solvents followed by light-absorption measurements using ultraviolet-visible (UV-vis) spectrophotometry (Chen and Bond 2010; Li, Chen, and Bond 2016). The main advantage of the online methods is the ability to retrieve the optical properties of the BrC aerosol while airborne. However, the retrieval process is relatively complex. The presence of BC, which is often co-emitted with BrC, induces relatively large uncertainty because retrieval calculations require knowledge of the poorly constrained BC mixing state and morphology (Saleh 2020; Stevens and Dastoor 2019). Since BC is insoluble in water and organic solvents (Bond et al. 2013), the offline methods have the advantage of isolating the BrC via solvent extraction. However, not all types of BrC are efficiently extracted in water and organic solvents (Corbin et al. 2019). Different types of BrC exhibit variable extraction efficiencies in different solvents, leading to retrieved light-absorption properties that are solvent-dependent (Chen and Bond 2010; Liu et al. 2013; Shetty et al. 2019).

Traditionally, the most widely used solvent to extract organic aerosol (OA) in atmospheric science research is water (Hecobian et al. 2010; Claeys et al. 2012; Zhang et al. 2013). Realizing that a significant fraction of OA is not water soluble, methanol has also been used as a solvent in more recent studies (Fuzzi and Decesari 2016; Xie et al. 2017; Xie, Hays, and Holder 2017; Phillips and Smith 2017). Methanol has been shown to be more effective at extracting OA in fresh combustion emissions (Chen and Bond 2010; Sengupta et al. 2018), which are relatively non-polar. Consequently, for the same combustion emissions, k values

retrieved for methanol-extracted BrC are larger than those for water-extracted BrC (Chen and Bond 2010; Wu et al. 2016). Some studies performed sequential extraction in water and methanol and reported overall absorption from the two extraction steps (Forrister et al. 2015; Liu et al. 2014; Chen and Bond 2010). Although relatively uncommon in atmospheric aerosol studies, dichloromethane (DCM) is frequently used as a solvent in combustion soot-formation research due to its efficacy at extracting the large-molecular-size polycyclic aromatic hydrocarbons (PAHs) that constitute nascent soot (Alfè et al. 2008; Apicella et al. 2007; Russo et al. 2013), which are important BrC components (Saleh et al. 2018; Cheng et al. 2020). BrC absorption (i.e., *k*) increases with increasing molecular size (Saleh et al. 2018) while its solubility decreases with increasing molecular size (Corbin et al. 2019). Therefore, offline solvent-extraction techniques are expected to underestimate BrC absorption as they miss the large-molecular-size S-BrC (Saleh 2020), which is poorly soluble or insoluble in organic solvents (Corbin et al. 2019). This is supported by the findings of Shetty et al. (2019) who reported that the extraction efficiency of biomass-burning BrC decreased with the increasing of BC/OA ratio, which is correlated with an increase in production of S-BrC (Cheng et al. 2019; Saleh 2020; Saleh et al. 2014).

In this study, we investigated the discrepancies in BrC light-absorption properties that arise from retrieval methods (online versus offline) and the choice of solvent in offline methods. We produced BrC with variable light-absorption properties from the controlled combustion of three structurally different fuels: toluene (aromatic), isooctane (branched alkane), and cyclohexane (cyclic alkane). We compared the BrC light-absorption properties retrieved from online measurements to those retrieved from offline solvent-extraction measurements using methanol and DCM as solvents.

2. Methods

2.1. Approach

We performed a systematic comparison between the light-absorption properties (k and w) of BrC retrieved from online light-absorption and aerosol size-distribution measurements and those retrieved from solvent-extraction followed by offline UV-vis spectrophotometry. We isolated three key effects:

- 1) Light-absorption properties of the suspended BrC particles: There is an association between BrC light-absorption properties and its physicochemical properties, such as solubility in organic solvents (Saleh 2020; Corbin et al. 2019). Therefore, it is important to assess the dependence of solvent-extraction bias on BrC light-absorption properties. To this effect, we generated BrC with variable k values that span the range observed for combustion BrC, including weakly absorbing BrC (W-BrC), moderately absorbing BrC (M-BrC), and strongly absorbing BrC (S-BrC) (Saleh 2020).
- 2) Fuel type: We used three structurally different fuels: toluene (aromatic), isooctane (branched alkane), and cyclohexane (cyclic alkane). For each fuel, we generated BrC spanning the optical classes described above and compared the solvent-extraction bias for BrC within the same optical class but produced from the different fuels.
- 3) Solvent type: We used two organic solvents: methanol and DCM. Methanol is recently becoming the most used organic solvent in atmospheric aerosol research. It has been shown or assumed to extract most or all (85%-100%) of the OA, including BrC (Chen and Bond 2010; Fuzzi and Decesari 2016; Sengupta et al. 2018; Xie, Hays, and Holder 2017; Cheng et al. 2016; Liu et al. 2013). On the other hand, DCM is commonly used in studies of organic nascent soot formation in combustion (Alfè et al. 2008; Apicella et al. 2007; Russo et al. 2013) due to its efficacy at extracting the PAHs that comprise the nascent soot. We

have previously shown that these PAHs constitute an important fraction of combustion BrC (Saleh et al. 2018); therefore, DCM can potentially be an appropriate solvent for atmospheric BrC research.

Details of the combustion experiments and the online and offline techniques employed to retrieved k and w of the generated BrC are described in the subsequent subsections.

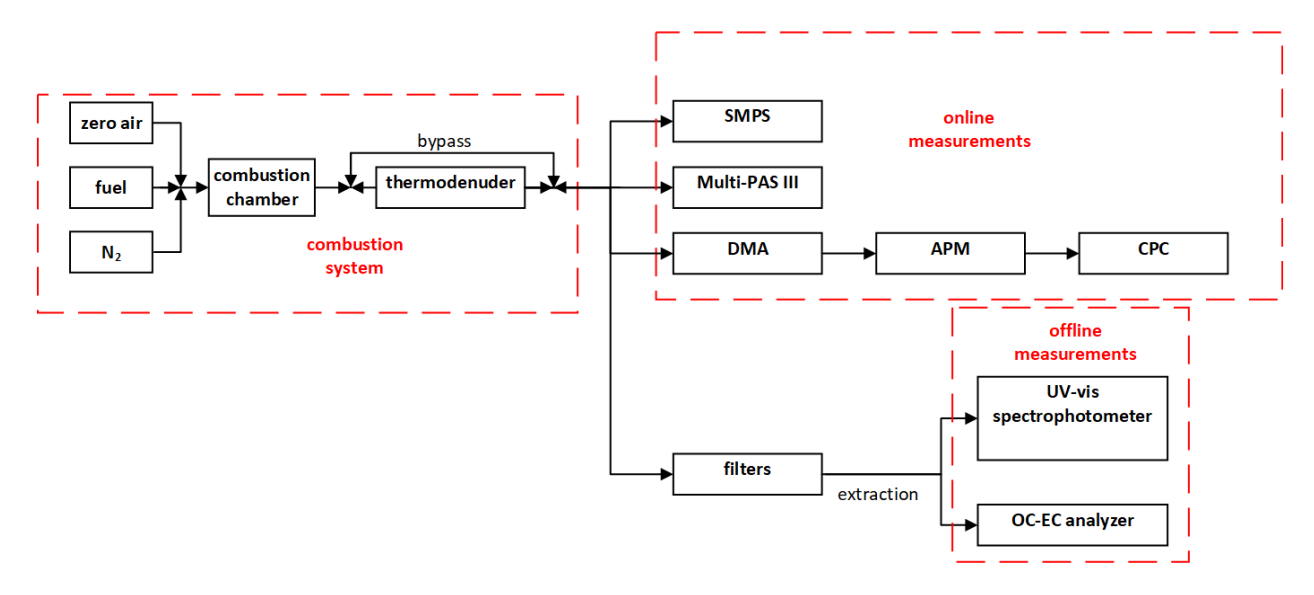


Figure 1. Schematic of the experimental setup.

2.2. Combustion experiments and online measurements

The combustion system utilized in this study is described in detail in Cheng et al. (2019). Briefly, controlled steady flows of fuel, clean air, and additional nitrogen (used as a passive diluent) were introduced into a temperature-controlled quartz combustion chamber. The temperature of the combustion chamber was controlled at either 950 °C or 1000 °C in these experiments. The fuel was introduced in vapor form using a bubbler at a flowrate dictated by the saturation vapor pressure of the fuel (3.4, 5.3, and 10.7 kPa for toluene, cyclohexane, and isooctane, respectively). The equivalence ratios in the experiments ranged between 1.1 and 4.7, and the nitrogen/oxygen ratio ranged between 1.9 and 80.5. By tuning the combustion conditions, we generated BrC with widely variable and well-controlled optical properties. In specific, increasing the combustion temperature, decreasing the equivalence ratio, and/or decreasing the nitrogen/oxygen ratio produces darker BrC (larger *k* and smaller *w*) (Saleh et al. 2018). In two experiments (one for cyclohexane and one for isooctane), dark BrC was further isolated by passing the emissions through a thermodenuder controlled at 120 °C. This process relies on the established association between volatility and BrC optical properties, namely that the residual (less volatile) fraction is darker than the evaporated (more volatile) fraction (Saleh et al. 2018, Saleh 2020). Details of the combustion conditions for each experiment are given in Table S1 in the Supplementary Information (SI).

In order to tune the combustion conditions to produce BrC of certain desired light-absorption properties, we relied on real-time calculations of the wavelength-dependent mass absorption cross-section (MAC, m^2 g⁻¹) and absorption Ångström exponent (AAE). Those could be readily obtained from the real-time measurements of the absorption coefficients (b_{abs} , Mm⁻¹) and total aerosol mass concentrations (m_p):

$$MAC(\lambda) = b_{abs}(\lambda)/m_p \tag{1}$$

AAE was obtained by fitting a power-law function to Equation (1). We measured b_{abs} at $\lambda = 422$, 532, and 781 nm using a 3-wavelength Multi-pass Photoacoustic Spectrophotometer Spectrometer (Multi-PAS III) (Fischer and Smith 2018). m_p was calculated by integrating the size distribution within the size range 10–550 nm measured using a scanning mobility particle sizer (SMPS, TSI) with a density value of 1.2 g cm⁻³, which was measured using the tandem differential mobility analyzer – aerosol particle mass analyzer (tandem DMA-APM) technique (Malloy et al. 2009). We classified the aerosols based on their electricity mobility diameter (d_m) using a differential mobility analyzer (DMA, TSI) and then measured the mass of the selected particles (m) using an aerosol particle mass (APM, Kanomax) analyzer. The mobility effective density (ρ_{eff}) was calculated as (McMurry et al. 2002):

$$\rho_{\text{eff}} = \frac{m}{\frac{\pi d_{\text{m}}^3}{6}} \tag{2}$$

We have previously confirmed that BrC particles formed at similar conditions were near-spherical particles based on scanning electron microscopy (SEM) images (Saleh et al. 2018). Thus, the mobility-equivalent volume of BrC particles in Equation (2) is equal to the true volume of the particles and $\rho_{\rm eff}$ measured by the tandem DMA-APM technique is equal to the true density. As shown by the calculations in the SI, the multiply charged particles contributed less than 1% of the particle mass and had a minimal effect on the retrieved effect densities.

For each experiment, we processed the light-absorption (Multi-PAS III) and size-distribution (SMPS) data to retrieve the BrC k at 422 nm, 532 nm, and 781 nm using optical closure (Saleh et al. 2018). Unlike MAC, k is independent of particle size, allowing for a direct comparison between the light-absorption properties of BrC in the aerosol phase with those of BrC extracts. The procedure involved optimizing a Mie code to reproduce the measured b_{abs} at each wavelength using the size distribution as input and k as a free parameter. We note that the combustion conditions were controlled to avoid BC production. We have previously shown that the pure organic particles generated under such conditions are near-spherical (Saleh, Cheng, and Atwi 2018), thus justifying the use of Mie calculations in the optical closure. Following the range of values reported in the literature, we assumed a real part of the refractive index between 1.5 and 1.7 in the calculations (Sumlin et al. 2018; Saleh et al. 2014; Moise, Flores, and Rudich 2015; Browne et al. 2019; Li, He, Hettiyadura, et al. 2019). We then calculated w as the exponent of a power-law fit to the retrieved k values versus wavelengths. Hereafter, we refer to the k and w values retrieved for the airborne particles as $k_{aerosol}$ and $w_{aerosol}$ to distinguish them from the k and w values retrieved from UV-vis measurements of extracts ($k_{extracts}$ and $k_{extracts}$).

2.3 Filter collection and extraction

For each experiment, we collected BrC samples at a flow rate of 10 lpm on 47 mm polytetrafluoroethylene (PTFE, Teflon) filters (Whatman, TE 35, 0.2 μ m pore size). To ensure we had enough BrC for clear UV-vis signals, we collected ~0.75 mg of BrC under each combustion condition, requiring approximately 3 hours of sampling time per condition. The combustion conditions and BrC optical properties were uniform during the sampling time, which is one of the main advantages of the combustion system employed in this study. In preliminary experiments, we noticed that the filters start clogging when loadings exceed ~0.3 mg. Thus, for each experiment, we collected three filters, each with a loading of ~0.25 mg.

The filter samples were extracted and analyzed immediately after collection in order to minimize any potential physicochemical changes. The filter extraction procedure was similar to Hecobian et al. (2010) and Phillips and Smith (2017). We divided each of the three filters into two pieces and sonicated one piece of each filter in a glass vial (Fisherbrand, 03-339-22F) for 20 minutes with 10 ml of either methanol

(Macron fine chemicals, 3016-16, \geq 99.8% purity) or DCM (SIGMA-ALDRICH, 270997-2L, \geq 99.8% purity). Preliminary experiments showed that sonication for longer than 20 minutes did not affect the results. After sonication, we filtered the solution using 0.2 μ m PTFE filters (STERLITECH Corporation, PTU021350, 13 mm diameter) to remove undissolved particles, which cause bias in the UV-vis absorption measurements due to scattering (Phillips and Smith 2017).

We estimated the BrC concentration in the solution (C_{BrC}) following a procedure similar to Li, Chen, and Bond (2016). We pipetted 300 µl from each solution using silicon-coated tips onto a blank prebaked 1.5 cm² quartz filter punch (Pall Inc., Tissuquartz 2500). We then evaporated the solvent using a 10 lpm stream of clean, dry air for 10 minutes. The BrC is orders of magnitude less volatile than the solvents (Boublik, Fried, Hala 1984), and therefore the amount of BrC evaporated in this procedure is negligible. The total mass of carbon on the filter punches (m_{TC}) was measured using an OC-EC analyzer (Sunset Laboratory Inc., Portland, OR, USA, Model 5L), and C_{BrC} was calculated as m_{TC} divided by the pipetted solution volume (300 µl). Even though in these experiments the OC as a whole exhibited substantial light absorption and is classified as BrC, it should be noted that OC is comprised of a range of species with variable lightabsorption properties, some of which might be negligibly absorbing in the visible spectrum. To validate the accuracy of this method, we prepared solutions with known concentrations of pyrene in DCM and methanol and were able to retrieve the concentrations with less than 7% error (see Table S2 in SI). With the absence of information on the elemental composition of the BrC, we assumed that the BrC concentration was equal to the carbon concentration. Based on previous chemical speciation measurements of BrC produced under similar conditions (Cheng et al. 2020), we expect OA/OC (or BrC/OC) to be close to 1 for the lightest BrC samples and less than 1.4 for the darkest BrC samples (Section 3.2).

It is important to note that control experiments that involved quantifying m_{TC} in solutions of extracted clean filters revealed that both methanol and DCM dissolved plastics (e.g., Polyvinyl chloride (PVC), polycarbonate (PC), polyethylene (PE)), which showed as an OC signal on the OCEC analyzer. To minimize the contact of the solvents with plastic, we used either metal or glass tools/containers in the extraction process and covered each vial with aluminum foil before sealing with the PVC cap. We verified that none of the tools/containers used in this extraction process caused any bias in the measured C_{BrC} (see SI). However, DCM still dissolved organic matter in the PTFE filters leading to ~ 0.026 g/l bias in C_{BrC} (see SI). Therefore, C_{BrC} in the DCM solutions was corrected by subtracting 0.026 g/l from the measured concentrations. We verified that the dissolved organic matter from the filters did not exhibit any UV-vis absorption.

2.4. Retrieving light-absorption properties of BrC extracts

The UV-vis absorbance (A) of the BrC extracts was measured in the range 200 nm to 800 nm at a 1 nm resolution using a UV-vis Spectrophotometer (Agilent, Cary 60). We retrieved the wavelength-dependent imaginary part of the refractive index of the extracts (k_{extracts}) from the measured absorbance following the method of Sun et al. (2007). k_{extracts} is related to the absorption coefficient of the BrC extracts (α , cm⁻¹):

$$k_{\text{extracts}}(\lambda) = \frac{\lambda}{4\pi}\alpha(\lambda)$$
 (3)

Note that even though α and b_{abs} have the same dimensions (L⁻¹), they have different physical meanings and should not be confused. While α is a material property, as evident in Equation (3), b_{abs} represents the total absorption cross-section of an aerosol per unit volume of air and therefore depends on the aerosol concentration. α is obtained from absorbance measurements as:

$$\alpha(\lambda) = \ln 10 \, \frac{A(\lambda)\rho}{c_{\rm BrC} \, L} \tag{4}$$

Where L is the optical path length (1 cm), C_{BrC} is the concentration of BrC extracts (Section 2.3), and ρ is the density of the extracted BrC, assumed to be 1.2 g cm⁻³ (the density we obtained for the suspended aerosol; Section 2.2). The derivation of Equations (3) and (4) are given in the SI.

The wavelength dependence of $k_{\text{exctracts}}$ (w_{extracts}) was obtained as the exponent of a power-law fit of $k_{\text{exctracts}}$ versus wavelength. For direct comparison between w_{aerosol} and w_{extracts} , the fit was limited to the wavelength range of the Multi-PAS III (422 nm – 781 nm). Note that since α is proportional to $k_{\text{extracts}}(\lambda)$ (Equation 3) and the wavelength dependence of α is AAE, it follows that AAE_{extracts} = w_{extracts} + 1, which is the expected relation for the small-particle limit (Saleh 2020). Furthermore, unlike k_{extracts} , the retrieval of w_{extracts} is independent of ρ and C_{BrC} and is thus not subject to the biases associated with the assumptions outlined above.

2.5. Validation of the online and offline methods using nigrosin

In order to quantify the bias in $k_{\rm exrtacts}$ and $w_{\rm extracts}$ associated with extraction efficiency, we need first to assess any inconsistency between the online (aerosol) and offline (extracts) retrieval methods that is not associated with extraction efficiency. To that effect, we compared $k_{\rm aerosol}$ and $k_{\rm extracts}$ of nigrosin (Sigma Aldrich, CAS# 8005-03-6), a water-soluble organic dye. Nigrosin has been widely used as a model material of light-absorbing aerosol to validate PAS measurements (Lack et al. 2006; Wiegand, Mathews, and Smith 2014; Bluvshtein et al. 2017). We prepared an aqueous solution of nigrosin and used a constant output atomizer (TSI 3076) followed by diffusion drying to generate nigrosin aerosol. We retrieved $k_{\rm aerosol}$ following the procedure described in Section 2.2 using a real part of the refractive index of 1.7 (Dinar et al. 2007). We retrieved $k_{\rm extracts}$ following the procedure described in Section 2.4 using a density of 1.5 g cm⁻³, which was obtained using the tandem DMA-APM technique.

3. Results and discussion

3.1. Light-absorption properties of nigrosin

Figure 2 shows k_{extracts} as a function of wavelength between 400 nm and 800 nm and k_{aerosol} at 422 nm, 532 nm, and 781 nm. We retrieved k_{aerosol} following the procedure described in Section 2.2. In the calculations, we used real part of the refractive index (n) values reported by Bluvshtein et al. (2017), which are 1.613 \pm 0.007, 1.641 \pm 0.007, and 1.836 \pm 0.011 at 422 nm, 532 nm, and 781 nm, respectively. Both online and offline retrievals show that k of nigrosin exhibits a peak in the mid-visible wavelengths and drops to smaller values towards the long-visible and short-visible wavelengths. This wavelength dependence of k is consistent with nigrosin's dark "midnight purple" appearance. At 532 nm, k_{aerosol} and k_{extracts} are 0.280 \pm 0.009 and 0.270 \pm 0.004, respectively, which are in good agreement, and within the range reported in the literature (Dinar et al. 2007; Garvey and Pinnick 1983; Bluvshtein et al. 2012; Lang-Yona et al. 2009; Bluvshtein et al. 2017) (Figure 2). The differences are larger at 422 nm ($k_{\text{aerosol}} = 0.160 \pm 0.004$, $k_{\text{extracts}} = 0.132 \pm 0.004$) and 781 nm ($k_{\text{aerosol}} = 0.207 \pm 0.006$, $k_{\text{extracts}} = 0.161 \pm 0.002$). Nevertheless, these results indicate that the light absorption properties obtained using online and offline methods are consistent, and any significant differences (> ~20%) in k_{aerosol} and k_{extracts} of BrC could be attributed to extraction efficiency.

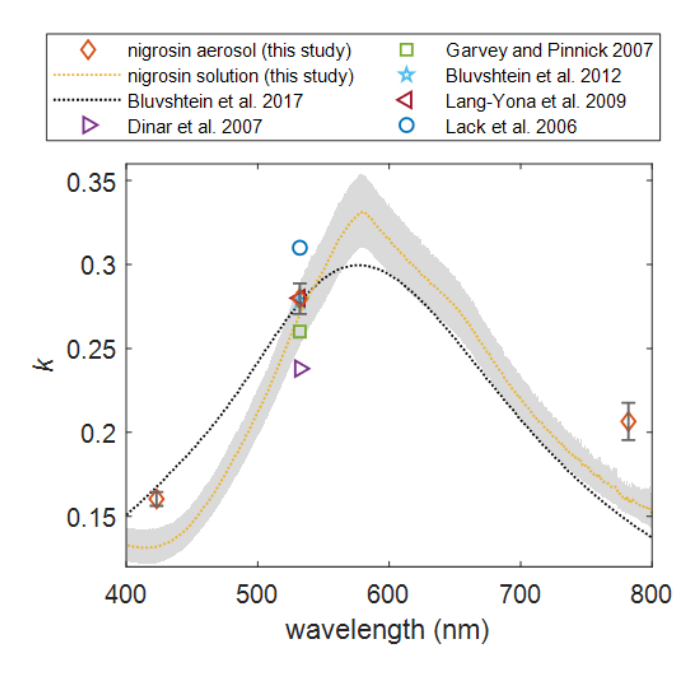


Figure 2. Imaginary part of the refractive index (k) of nigrosin retrieved from online and offline measurements. The range of the shaded area is the uncertainty of UV-vis measurements (~5%), which is a combination of the variances of the absorption measurements and uncertainty in the concentration measurements (see uncertainty analysis in SI). The error bars reflect the uncertainty in online measurements (absorption coefficients and size distributions) and the range of n values used in Mie calculations.

3.2 Comparison of the light-absorption properties of BrC aerosol and extracts

The BrC generated from the controlled combustion of toluene, cyclohexane, and isooctane had k_{aerosol} at 532 nm ($k_{\text{aerosol},532}$) values ranging over approximately two orders of magnitude (0.005 to 0.127). These values cover the range for combustion BrC reported in the literature, and fall under the weakly absorbing (W-BrC), moderately absorbing (M-BrC), and strongly absorbing (S-BrC) optical-based classes introduced by Saleh (2020). $w_{\text{aerosol},532}$ exhibit an inverse relation, where darker BrC is characterized by larger $k_{\text{aerosol},532}$ and smaller w_{aerosol} (Saleh et al. 2018), consistent with the darker BrC being composed of larger molecular-size aromatic species with smaller optical energy gaps that extend their absorption into longer wavelengths (Corbin et al. 2019). The corresponding w_{aerosol} ranged between 3.0 and 9.2 for the darkest and lightest BrC, respectively. The numerical values of k_{aerosol} and w_{aerosol} from all experiments are given in Table S1 in the SI.

The BrC concentrations (C_{BrC}) and UV-vis absorbance of BrC extracts in the two solvents are plotted against $k_{aerosol,532}$ in Figure 3. As shown in Figure 3a, with the exception of the lightest BrC sample (smallest $k_{aerosol,532}$), C_{BrC} of the DCM extracts was larger than C_{BrC} of the methanol extracts, indicating that DCM had a better extraction efficiency than methanol based on carbon mass. The significance of the difference in extraction efficiency between the two solvents is more evident in Figure 3b, which shows relatively close absorbances of DCM and methanol extracts for the light BrC samples (small $k_{aerosol,532}$) but a significantly steeper increase in the absorbance of DCM extracts with increasing $k_{aerosol,532}$ compared to methanol extracts. Absorbance is a consequence of both abundance (i.e., C_{BrC}) and intrinsic absorption (i.e., k), as evident in Equation 3 and Equation 4. Therefore, these results indicate that for the same BrC aerosol, the DCM extracts did not only have higher BrC mass concentrations, but the BrC in DCM extracts was also more absorbing (darker) than the BrC in methanol extracts. We note that since the DCM extracts are darker and are thus

expected to exhibit larger molecular sizes than methanol extracts (Saleh, Cheng, and Atwi 2018), the better carbon-mass-based extraction efficiency of DCM might not necessarily translate to better extraction efficiency in terms of number of molecules. The results in Figure 3 indicate that a small fraction of highly absorbing BrC molecules contributes disproportionately to overall BrC absorption. For instance, the concentration of DCM extracts of the darkest BrC sample is a factor of 2 larger than the methanol extracts, but their absorbance is larger by a factor of 5.

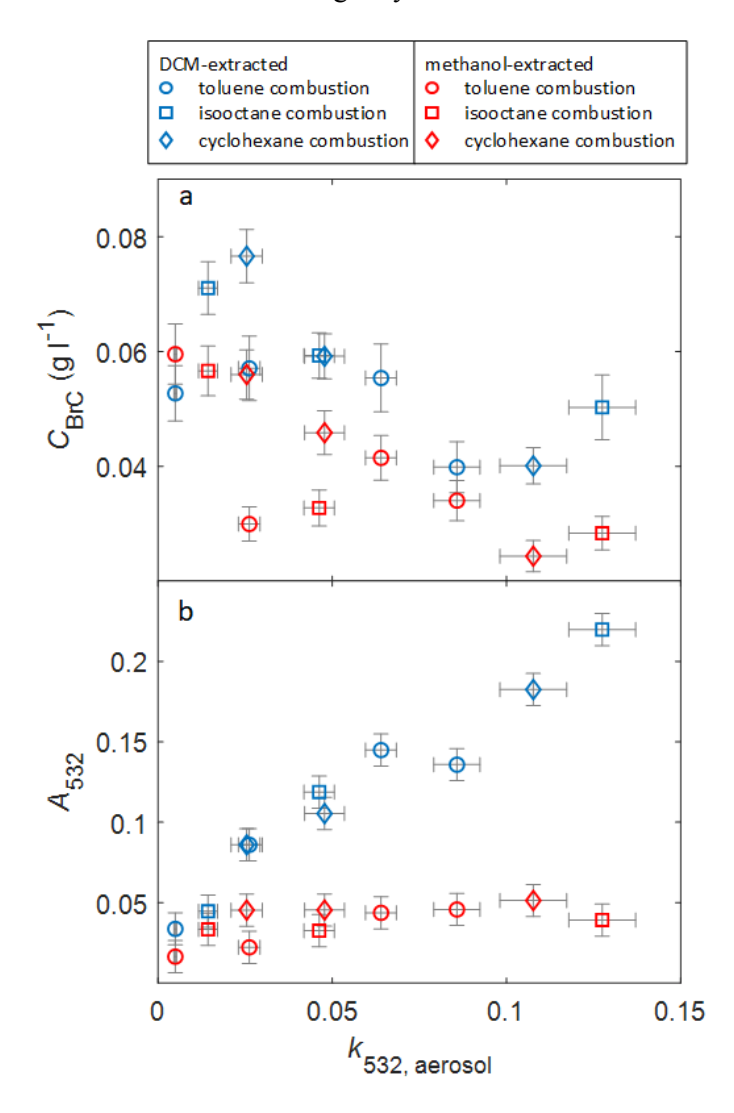


Figure 3. Comparisons of (a) concentrations ($C_{\rm BrC}$) and (b) absorbance at 532 nm (A_{532}) of DCM-extracted and methanol-extracted BrC as a function of the imaginary part of the refractive index of BrC aerosol at 532 nm $k_{\rm aerosol,532}$. BrC was generated from the combustion of toluene, cyclohexane, and isooctane. Error bar represent measurement uncertainties (see uncertainties analysis in SI). The horizontal error bars reflect the uncertainty in online measurements (absorption coefficients and size distributions) and the uncertainty associated with the range of n values used in Mie calculations. The uncertainty analysis associated with concentration and absorption measurements (vertical error bars) are described in the SI.

This is further illustrated in Figure 4, which depicts $k_{\text{extracts},532}$ and w_{extracts} obtained from the offline solvent-extraction measurements using methanol and DCM plotted against $k_{\text{aerosol},532}$ and w_{aerosol} . The numerical values of $k_{\text{extracts},532}$ and w_{extracts} from all experiments are given in Table S1 in the SI. Also, the

spectra of k_{extracts} and k_{aerosol} versus wavelength from all experiments are plotted in Figure S2 in the SI. We note that even though the combustion conditions are controlled in this study and the BrC produced at each condition is relatively uniform compared to real-life uncontrolled combustion, the BrC at each condition still comprises species with a continuum of molecular sizes and light-absorption properties. As evident in Figure 4, the DCM-extracted BrC was darker (larger $k_{\text{extracts},532}$ and smaller w_{extracts}) than the methanol-extracted BrC, indicating that DCM was more efficient at extracting the larger-molecular-size, more light-absorbing fraction of the BrC. There is no apparent fuel dependence of the difference in light-absorption properties between methanol-extracted and DCM-extracted BrC, suggesting that there is no significant fuel dependence of the difference in extraction efficiency between methanol and DCM. These results indicate that DCM is a more potent solvent than methanol in extracting combustion BrC, particularly the darker fraction. Given that the absorbances (Figure 3) and light-absorption properties (Figure 4) of the DCM and methanol extracts are similar for W-BrC and diverge as BrC becomes darker, we expect the methanol extracts are a subset of DCM extracts. However, it is possible that some molecules are extracted by methanol and not DCM, in which case sequential extraction in both solvents would lead to better BrC quantification.

With the exception of the lightest BrC data point (Figure 4), the BrC from all fuels and combustion conditions had $k_{\rm exrtacts} < k_{\rm aerosol}$ and $w_{\rm extracts} > w_{\rm aerosol}$ for both solvents, signifying that, even with DCM, the extraction efficiency of each BrC sample was lower for the darker fraction of the sample. This is expected because, for some classes of molecules, solubility decreases with increasing molecular size (Corbin et al. 2019), while BrC absorption increases with molecular size (Saleh et al. 2018). These results are consistent with the findings of Shetty et al. (2019) who compared light absorption by biomass-burning BrC aerosol to light absorption by BrC extracts using water, methanol and acetone. They reported that, for all solvents, the ratio of extracts absorption to aerosol absorption decreased with increasing BC/OA of the emissions, which is correlated with increasing BrC darkness (Saleh et al. 2014; Cheng et al. 2019; McClure et al. 2020).

In general, the results shown in Figure 4 show that solvent-extraction techniques can substantially underestimate BrC light absorption. For methanol-extracted BrC, kextracts 532 was smaller than 0.025 and w_{extracts} was larger than 7 for all samples, suggesting that the majority of methanol-extracted BrC was weakly absorbing (W-BrC). On the other hand, DCM also extracted a significant fraction of the moderately absorbing BrC (M-BrC), but the strongly absorbing BrC (S-BrC) remained largely unextracted. The BrC in this study was produced from the combustion of single-molecule fuels and does not exhibit the diversity in molecular structures of combustion BrC in the atmosphere. However, we expect that the general trends observed in this study, namely the dependence of solubility on optical class and the associated discrepancy between offline solvent-extraction and online methods, to apply to combustion BrC in general. Real-life uncontrolled combustion (e.g., biomass burning) produces BrC components that exhibit wide distributions within different optical classes, with the fraction of components in each class being dependent on the general combustion regime. Smoldering combustion would feature more of the W-BrC class, while flaming combustion would feature more of the M-BrC and S-BrC classes (Saleh 2020). Therefore, as can be inferred from Figure 4, the bias in BrC light-absorption properties retrieved from solvent-extraction methods is expected to become more prominent as the combustion approaches flaming conditions and the emitted BrC becomes darker.

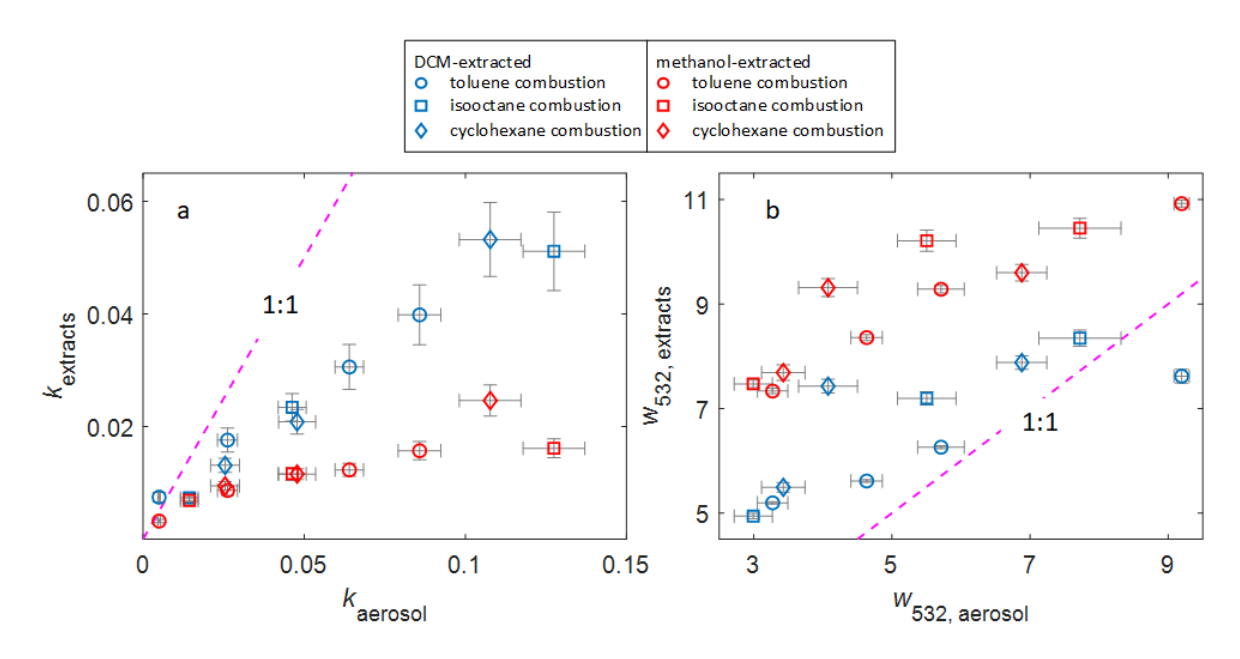


Figure 4. Comparison of BrC light-absorption properties retrieved from online measurements (aerosol) and offline measurements (extracts) using methanol and DCM as solvents. For clarity, uncertainty bounds (given in Table S1) are not shown in the figure. a) Imaginary part of the refractive indices at 532 nm. b) Wavelength dependence of the imaginary part of the refractive indices. The horizontal error bars reflect the uncertainty in online measurements (absorption coefficients and size distributions) and the uncertainty associated with the range of *n* values used in Mie calculations. The vertical error bars reflect a combination of the variances of the absorption measurements and uncertainty in the concentration measurements (see uncertainty analysis in SI).

3.3 The continuum of light-absorption properties

We have previously established that BrC exhibits a continuum of light-absorption properties characterized by pairs of inversely correlated mid-visible k (e.g., k at 550 nm, k_{550}) and its wavelength dependence (w), where k_{550} and w approach those of BC for the darkest BrC on the continuum (Saleh et al. 2018). In that study, we generated BrC from the combustion of benzene and toluene and retrieved the light-absorption properties from online measurements (same procedure as Section 2.2). In this study, we further expanded the data set by 1) generating BrC from two additional structurally different fuels (cyclohexane and isooctane) and 2) retrieving k_{550} and w of BrC extracts using methanol and DCM as solvents in addition to k_{550} and w of the aerosol. All the w versus k_{550} data points from this study and Saleh et al. (2018) are plotted in Figure 5. The k_{550} values of BrC aerosols from this study were calculated from the k_{532} retrieved from the online b_{abs} measurements at 532 nm and w values (Figure 4) as $k_{550} = k_{532}$ (532/550) w .

As shown in Figure 5, regardless of structural difference (branched alkane, cycloalkane, aromatic), BrC from all three fuels reproduced the brown-black continuum introduced by Saleh et al. (2018) with well-correlated k_{550} and w. This result further confirms that BrC production and its light-absorption properties are not tied to certain fuel types, but are governed by combustion conditions (Saleh et al. 2018; Saleh 2020; Cheng et al. 2019). The combustion of any hydrocarbon fuel can produce BrC at any location along the brown-black continuum if combusted at the "right" combustion conditions (temperature, equivalence ratio). However, these right conditions are different for different fuels (Cheng et al. 2019; Saleh 2020).

Even though the solvents, especially methanol, only extracted the less-absorbing fraction of the BrC samples, the k_{550} and w of the extracts still fall on the same continuum as those of the BrC aerosol. This provides further evidence for the inverse relation between k_{550} and w of BrC. Furthermore, these results provide support for the conclusion that the differences observed between k_{aerosol} and k_{extracts} (Figure 4) are due to the inefficiency of solvent extraction and not due to intrinsic differences between the online and offline methods.

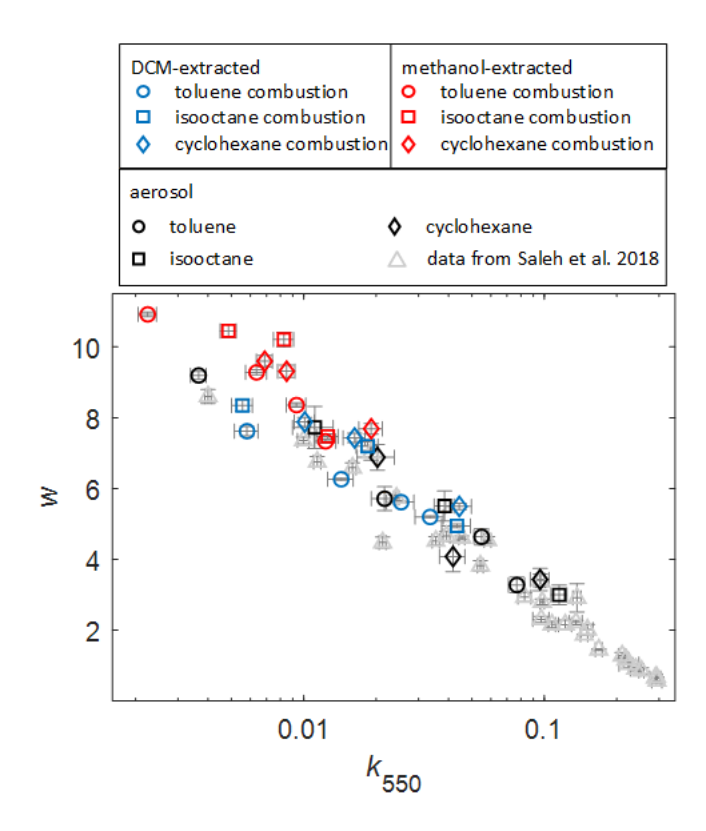


Figure 5. Wavelength dependence of the imaginary part of the refractive index (w) versus the imaginary part of the refractive index at 550 nm (k_{550}) of BrC generated from controlled-combustion of toluene, isooctane, and cyclohexane. The k_{550} and w values include those retrieved from online measurements (aerosol) and offline measurements using solvent-extraction by DCM and methanol (extracts). Also shown are k_{550} and w values from Saleh et al. (2018) for BrC aerosol produced from the combustion of toluene and benzene.

4. Conclusions

The experiments performed in this study revealed significant discrepancies between BrC light-absorption properties retrieved using online methods and offline solvent-extraction methods. These discrepancies are mainly associated with extraction inefficiency, which is more prominent for darker BrC. For the BrC produced in this study from the combustion of toluene, cyclohexane, and isooctane, DCM exhibited better extraction efficiency, and thus less bias in retrieved light-absorption properties, than methanol, indicating that DCM is a more powerful solvent for extracting combustion BrC. However, even with DCM, the imaginary part of the refractive indices of the extracts were significantly smaller than those of the aerosol, with the difference increasing with increasing BrC darkness. Therefore, it should be noted that BrC light-absorption properties obtained using offline solvent-extraction techniques are those of the extracted fraction and are not necessarily representative of the whole BrC. The results obtained in this study also provide further evidence that BrC exhibits a continuum of light-absorption properties characterized by pairs of

inversely correlated mid-visible imaginary part of the refractive indices (e.g., at 550 nm, k_{550}) and their wavelength dependence (w). The inverse correlation between k_{550} and w applies for BrC produced from the combustion of structurally different fuels and for k_{550} and w obtained from both online and offline solvent-extraction techniques.

Funding

Financial support was provided by the National Science Foundation, Division of Atmospheric and Geospace Sciences (AGS-1748080) and the University of Georgia Interdisciplinary Seed Grant Initiative.

References:

- Adler, G., N. L. Wagner, K. D. Lamb, K. M. Manfred, J. P. Schwarz, A. Franchin, A. M. Middlebrook, et al. 2019. Evidence in Biomass Burning Smoke for a Light- Absorbing Aerosol with Properties Intermediate between Brown and Black Carbon. *Aerosol Science and Technology* 53 (9): 976–89. doi.org/10.1080/02786826.2019.1617832.
- Alfè, M., B. Apicella, A. Tregrossi, and A. Ciajolo. 2008. Identification of Large Polycyclic Aromatic Hydrocarbons in Carbon Particulates Formed in a Fuel-Rich Premixed Ethylene Flame. *Carbon* 46 (15): 2059–66. doi.org/10.1016/j.carbon.2008.08.019.
- Andreae, M. O., and A. Gelencsér. 2006. Black Carbon or Brown Carbon? The Nature of Light-Absorbing Carbonaceous Aerosols. *Atmos. Chem. Phys.* 6 (10): 3131–48. doi.org/10.5194/acp-6-3131-2006.
- Apicella, B., A. Carpentieri, M. Alfè, R. Barbella, A. Tregrossi, P. Pucci, and A. Ciajolo. 2007. Mass Spectrometric Analysis of Large PAH in a Fuel-Rich Ethylene Flame. *Proceedings of the Combustion Institute* 31: 547–53. doi.org/10.1016/j.proci.2006.08.014.
- Bluvshtein, N., J. M. Flores, A. A. Riziq, Y. Rudich, N. Bluvshtein, J. M. Flores, A. A. Riziq, and Y. Rudich. 2012. An Approach for Faster Retrieval of Aerosols' Complex Refractive Index Using Cavity Ring-Down Spectroscopy. *Aerosol Science and Technology* 46 (10): 1140–1150. doi.org/10.1080/02786826.2012.700141.
- Bluvshtein, N., J. M. Flores, Q. He, E. Segre, L. Segev, N. Hong, A. Donohue, J. N. Hilfiker, and Y. Rudich. 2017. Calibration of a Multi-Pass Photoacoustic Spectrometer Cell Using Light-Absorbing Aerosols. *Atmos. Meas. Tech.* 10: 1203–13. doi.org/10.5194/amt-10-1203-2017.
- Bond, T. C., S. J. Doherty, D. W. Fahey, P. M. Forster, T. Berntsen, B. J. Deangelo, M. G. Flanner, et al. 2013. Bounding the Role of Black Carbon in the Climate System: A Scientific Assessment. *Geophysical Research Atmospheres* 118 (11): 5380–5552. doi.org/10.1002/jgrd.50171.
- Browne, E. C., X. Zhang, J. P. Franklin, K. J. Ridley, T. W. Kirchstetter, K. R. Wilson, C. D. Cappa, and J. H. Kroll. 2019. Effect of Heterogeneous Oxidative Aging on Light Absorption by Biomass Burning Organic Aerosol. *Aerosol Science and Technology* 53 (6): 663–74. doi.org/10.1080/02786826.2019.1599321.
- Chakrabarty, R. K., H. Moosmüller, L. W. A. Chen, K. Lewis, W. P. Arnott, C. Mazzoleni, M. K. Dubey, et al. 2010. Brown Carbon in Tar Balls from Smoldering Biomass Combustion. *Atmos. Chem. Phys.* 10 (13): 6363–70. doi.org/10.5194/acp-10-6363-2010.
- Chen, Y., and T. C. Bond. 2010. Light Absorption by Organic Carbon from Wood Combustion. *Atmos. Chem. Phys.* 9 (2001): 20471–513. doi.org/10.5194/acpd-9-20471-2009.
- Cheng, Y., K. He, Z. Du, G. Engling, J. Liu, Y. Ma, M. Zheng, and R. J. Weber. 2016. The Characteristics of Brown Carbon Aerosol during Winter in Beijing. *Atmospheric Environment* 127: 355–64. doi.org/10.1016/j.atmosenv.2015.12.035.
- Cheng, Z., K. M. Atwi, Z. Yu, A. Avery, C. Fortner, L. Williams, F. Majluf, J. E. Krechmer, and A. T. Lambe. 2020. Evolution of the Light-Absorption Properties of Combustion Brown Carbon Aerosols Following Reaction with Nitrate Radicals. *Aerosol Science and Technology* 0 (0): 1–15. doi.org/10.1080/02786826.2020.1726867.
- Cheng, Z., K. Atwi, T. Onyima, and R. Saleh. 2019. Investigating the Dependence of Light-Absorption Properties of Combustion Carbonaceous Aerosols on Combustion Conditions. *Aerosol Science and Technology* 53 (4): 419–34. doi.org/10.1080/02786826.2019.1566593.
- Chylek, P., J. E. Lee, D. E. Romonosky, F. Gallo, S. Lou, M. Shrivastava, C. M. Carrico, A. C. Aiken,

- and M. K. Dubey. 2019. Mie Scattering Captures Observed Optical Properties of Ambient Biomass Burning Plumes Assuming Uniform Black, Brown, and Organic Carbon Mixtures. *J. Geophys. Res. Atmos* 124 (21): 11406–27. doi.org/10.1029/2019JD031224.
- Claeys, M., R. Vermeylen, F. Yasmeen, Y. Gómez-González, X. Chi, W. Maenhaut, T. Mészáros, and I. Salma. 2012. Chemical Characterisation of Humic-like Substances from Urban, Rural and Tropical Biomass Burning Environments Using Liquid Chromatography with UV/Vis Photodiode Array Detection and Electrospray Ionisation Mass Spectrometry. *Environ. Chem.* 9 (3): 273–84. doi.org/10.1071/EN11163.
- Corbin, J. C., H. Czech, D. Massabò, F. B. de Mongeot, G. Jakobi, F. Liu, P. Lobo, et al. 2019. Infrared-Absorbing Carbonaceous Tar Can Dominate Light Absorption by Marine-Engine Exhaust. *Npj Climate and Atmospheric Science* 2 (1). doi.org/10.1038/s41612-019-0069-5.
- Desyaterik, Y., Y. Sun, X. Shen, T. Lee, X. Wang, T. Wang, and J. L. C. Jr. 2013. Speciation of "Brown" Carbon in Cloud Water Impacted by Agricultural Biomass Burning in Eastern China. *J. Geophys. Res. Atmos.* 118: 7389–99. doi.org/10.1002/jgrd.50561.
- Dinar, E., A. Abo Riziq, C. Spindler, C. Erlick, G. Kiss, and Y. Rudich. 2007. The Complex Refractive Index of Atmospheric and Model Humic-like Substances (HULIS) Retrieved by a Cavity Ring down Aerosol Spectrometer (CRD-AS). *The Royal Society of Chemistry* 137: 279–95. doi.org/10.1039/b703111d.
- Feng, Y., V. Ramanathan, and V. R. Kotamarthi. 2013. Brown Carbon: A Significant Atmospheric Absorber of Solar Radiation? *Atmos. Chem. Phys.* 13 (17): 8607–21. doi.org/10.5194/acp-13-8607-2013.
- Fischer, D. A., and G. D. Smith. 2018. A Portable, Four-Wavelength, Single-Cell Photoacoustic Spectrometer for Ambient Aerosol Absorption. *Aerosol Science and Technology* 52 (4): 393–406. doi.org/10.1080/02786826.2017.1413231.
- Forrister, H., J. Liu, E. Scheuer, J. Dibb, L. Ziemba, K. L. Thornhill, B. Anderson, et al. 2015. Evolution of Brown Carbon in Wildfire Plumes. *Geophys. Res. Lett.* 42: 4623–30. doi.org/10.1002/2015GL063897.Received.
- Fuzzi, S., and S. Decesari. 2016. Light Absorption Properties of Brown Carbon in the High Himalayas. *J. Geophys. Res. Atmos.* 121: 9621–39. doi.org/10.1002/2016JD025030.Received.
- Garvey, D. M., and R. G. Pinnick. 1983. Response Characteristics of the Particle Measuring Systems Active Scattering Aerosol Spectrometer Probe (ASASP–X). *Aerosol Science and Technology* 2 (4): 477–88. doi.org/10.1080/02786828308958651.
- Hammer, M. S., R. V Martin, A. Van Donkelaar, V. Buchard, O. Torres, D. A. Ridley, and R. J. D. Spurr. 2016. Interpreting the Ultraviolet Aerosol Index Observed with the OMI Satellite Instrument to Understand Absorption by Organic Aerosols: Implications for Atmospheric Oxidation and Direct Radiative Effects. *Atmos. Chem. Phys.* 16: 2507–23. doi.org/10.5194/acp-16-2507-2016.
- Hecobian, A., X. Zhang, M. Zheng, N. Frank, E. S. Edgerton, R. J. Weber, A. Sciences, T. Park, and N. Carolina. 2010. Water-Soluble Organic Aerosol Material and the Light-Absorption Characteristics of Aque- Ous Extracts Measured Over the Southeastern United States. Atmos. *Atmos. Chem. Phys.* 10: 5965–77. doi.org/10.5194/acp-10-5965-2010.
- Jo, D. S., R. J. Park, S. Lee, S. Kim, and X. Zhang. 2016. A Global Simulation of Brown Carbon: Implications for Photochemistry and Direct Radiative Effect. *Atmos. Chem. Phys.* 16: 3413–32. doi.org/10.5194/acp-16-3413-2016.
- Kampf, C. J., A. Filippi, C. Zuth, T. Hoffmann, and T. Opatz. 2016. Secondary Brown Carbon Formation via the Dicarbonyl Imine Pathway: Nitrogen Heterocycle Formation and Synergistic Effect. *Phys. Chem. Chem. Phys.* 18: 18353–64. doi.org/10.1039/c6cp03029g.

- Lack, D. A., J. M. Langridge, R. Bahreini, C. D. Cappa, A. M. Middlebrook, and J. P. Schwarz. 2012. Brown Carbon and Internal Mixing in Biomass Burning Particles. *PNAS* 109 (37): 14802–7. doi.org/10.1073/pnas.1206575109.
- Lack, D. A., E. R. Lovejoy, T. Baynard, A. Pettersson, and A. R. Ravishankara. 2006. Aerosol Absorption Measurement Using Photoacoustic Spectroscopy: Sensitivity, Calibration, and Uncertainty Developments. *Aerosol Science and Technology* 40 (9): 697–708. doi.org/10.1080/02786820600803917.
- Lang-Yona, N., Y. Rudich, E. Segre, E. Dinar, and A. Abo-Riziq. 2009. Complex Refractive Indices of Aerosols Retrieved by Continuous Wave-Cavity Ring Down Aerosol. *Anal. Chem.* 81 (16): 1762–69.
- Laskin, A., J. Laskin, and S. A. Nizkorodov. 2015. Chemistry of Atmospheric Brown Carbon. *Chemical Reviews* 115 (10): 4335–82. doi.org/10.1021/cr5006167.
- Li, C., Q. He, A. P. S. Hettiyadura, U. Käfer, G. Shmul, D. Meidan, R. Zimmermann, et al. 2019. Formation of Secondary Brown Carbon in Biomass Burning Aerosol Proxies through NO3 Radical Reactions. *Environ. Sci. Technol.* 54 (3): 1395–1405. doi.org/10.1021/acs.est.9b05641.
- Li, C., Q. He, J. Schade, J. Passig, R. Zimmermann, D. Meidan, A. Laskin, and Y. Rudich. 2019. Dynamic Changes in Optical and Chemical Properties of Tar Ball Aerosols by Atmospheric Photochemical Aging. *Atmos. Chem. Phys.* 19: 139–63. doi.org/10.5194/acp-19-139-2019.
- Li, X., Y. Chen, and T. C. Bond. 2016. Light Absorption of Organic Aerosol from Pyrolysis of Corn Stalk. *Atmospheric Environment* 144: 249–56. doi.org/10.1016/j.atmosenv.2016.09.006.
- Liu, D., J. Whitehead, M. R. Alfarra, E. Reyes-Villegas, D. V. Spracklen, C. L. Reddington, S. Kong, et al. 2017. Black-Carbon Absorption Enhancement in the Atmosphere Determined by Particle Mixing State. *Nature Geoscience* 10 (3): 184–88. doi.org/10.1038/ngeo2901.
- Liu, J, M. Bergin, H. Guo, L. King, N. Kotra, E. Edgerton, and R. J. Weber. 2013. Size-Resolved Measurements of Brown Carbon in Water and Methanol Extracts and Estimates of Their Contribution to Ambient Fine-Particle Light Absorption. *Atmos. Chem. Phys.* 13: 12389–404. doi.org/10.5194/acp-13-12389-2013.
- Liu, J., P. Lin, A. Laskin, J. Laskin, S. M. Kathmann, M. Wise, R. Caylor, et al. 2016. Optical Properties and Aging of Light-Absorbing Secondary Organic Aerosol. *Atmos. Chem. Phys.* 16 (19): 12815–27. doi.org/10.5194/acp-16-12815-2016.
- Liu, J., E. Scheuer, J. Dibb, L. D. Ziemba, K. L. Thornhill, B. E. Anderson, A. Wisthaler, et al. 2014. Brown Carbon in the Continental Troposphere. *Geophys. Res. Lett.* 41: 2191–95. doi.org/10.1002/2013GL058976.Received.
- Malloy, Q. G. J., S. Nakao, L. Qi, R. Austin, C. Stothers, H. Hagino, and D. R. Cocker. 2009. Real-Time Aerosol Density Determination Utilizing a Modified Scanning Mobility Particle Sizer Aerosol Particle Mass Analyzer System. *Aerosol Science and Technology* 43 (7): 673–78. doi.org/10.1080/02786820902832960.
- Marrero-Ortiz, W., M. Hu, Z. Du, Y. Ji, Y. Wang, S. Guo, Y. Lin, et al. 2019. Formation and Optical Properties of Brown Carbon from Small α-Dicarbonyls and Amines. *Environ. Sci. Technol.* 53 (1): 117–26. doi.org/10.1021/acs.est.8b03995.
- McClure, C. D., C. Y. Lim, D. H. Hagan, J. H. Kroll, and C. D. Cappa. 2020. Biomass-Burning-Derived Particles from a Wide Variety of Fuels Part 1: Properties of Primary Particles. *Atmospheric Chemistry and Physics* 20 (3): 1531–47. doi.org/10.5194/acp-20-1531-2020.
- McMurry, P. H., X. Wang, K. Park, and K. Ehara. 2002. The Relationship between Mass and Mobility for Atmospheric Particles: A New Technique for Measuring Particle Density. *Aerosol Science and*

- Technology 36 (2): 227–38. doi.org/10.1080/027868202753504083.
- Moise, T., J. M. Flores, and Y. Rudich. 2015. Optical Properties of Secondary Organic Aerosols and Their Changes by Chemical Processes. *Chem. Rev.* 115: 4400–4439. doi.org/10.1021/cr5005259.
- Phillips, S. M., and G. D. Smith. 2014. Light Absorption by Charge Transfer Complexes in Brown Carbon Aerosols. *Environ. Sci. Technol. Lett.* 1 (10): 382–86. doi.org/10.1021/ez500263j.
- ——. 2015. Further Evidence for Charge Transfer Complexes in Brown Carbon Aerosols from Excitation-Emission Matrix Fluorescence Spectroscopy. *J. Phys. Chem.* 119 (19): 4545–51. doi.org/10.1021/jp510709e.
- Phillips, S. M., and G. D. Smith. 2017. Spectroscopic Comparison of Water- and Methanol-Soluble Brown Carbon Particulate Matter. *Aerosol Science and Technology* 51 (9): 1113–1121. doi.org/10.1080/02786826.2017.1334109.
- Russo, C., M. Alfe, J. N. Rouzaud, F. Stanzione, A. Tregrossi, and A. Ciajolo. 2013. Probing Structures of Soot Formed in Premixed Flames of Methane, Ethylene and Benzene. *Proceedings of the Combustion Institute* 34 (1): 1885–92. doi.org/10.1016/j.proci.2012.06.127.
- Saleh, R., C. J. Hennigan, G. R. McMeeking, W. K. Chuang, E. S. Robinson, H. Coe, N. M. Donahue, and A. L. Robinson. 2013. Absorptivity of Brown Carbon in Fresh and Photo-Chemically Aged Biomass-Burning Emissions. *Atmos. Chem. Phys.* 13: 7683–93. doi.org/10.5194/acp-13-7683-2013.
- Saleh, R.. 2020. From Measurements to Models: Toward Accurate Representation of Brown Carbon in Climate Calculations. *Curr Pollution Rep*, no. 706. doi.org/doi.org/10.1007/s40726-020-00139-3.
- Saleh, R., Z. Cheng, and K. Atwi. 2018. The Brown–Black Continuum of Light-Absorbing Combustion Aerosols. Rapid-communication. *Environ. Sci. Technol. Lett.* 5: 508–13. doi.org/10.1021/acs.estlett.8b00305.
- Saleh, R., M. Marks, J. Heo, P. J. Adams, N. M. Donahue, and A. L. Robinson. 2015. Contribution of Brown Carbon and Lensing to the Direct Radiative Effect of Carbonaceous Aerosols from Biomass and Biofuel Burning Emissions. *J. Geophys. Res. Atmos* 120 (10): 10,285–10,296. doi.org/10.1002/2015JD023697.
- Saleh, R., E. S. Robinson, D. S. Tkacik, A. T. Ahern, S. Liu, A. C. Aiken, R. C. Sullivan, et al. 2014. Brownness of Organics in Aerosols from Biomass Burning Linked to Their Black Carbon Content. *Nature Geoscience* 7 (9): 647–50. doi.org/10.1038/ngeo2220.
- Sengupta, D., V. Samburova, C. Bhattarai, E. Kirillova, L. Mazzoleni, M. Iaukea-Lum, A. Watts, H. Moosmüller, and A. Khlystov. 2018. Light Absorption by Polar and Non-Polar Aerosol Compounds from Laboratory Biomass Combustion. *Atmospheric Chemistry and Physics* 18 (15): 10849–67. doi.org/10.5194/acp-18-10849-2018.
- Shetty, N. J., A. Pandey, S. Baker, W. M. Hao, and R. K. Chakrabarty. 2019. Measuring Light Absorption by Freshly Emitted Organic Aerosols: Optical Artifacts in Traditional Solvent-Extraction-Based Methods. *Atmos. Chem. Phys.* 19: 8817–30.
- Stevens, R., and A. Dastoor. 2019. A Review of the Representation of Aerosol Mixing State in Atmospheric Models. *Atmosphere* 10 (4). doi.org/10.3390/atmos10040168.
- Sumlin, B. J., C. Oxford, B. Seo, R. Pattison, B. J. Williams, and R. K. Chakrabarty. 2018. Density and Homogeneous Internal Composition of Primary Brown Carbon Aerosol. *Environ. Sci. Technol.*, no. 1: acs.est.8b00093. doi.org/10.1021/acs.est.8b00093.
- Sun, H., L. Biedermann, and T. C. Bond. 2007. Color of Brown Carbon: A Model for Ultraviolet and Visible Light Absorption by Organic Carbon Aerosol. *Geophys. Res. Lett.* 34: L17813. doi.org/10.1029/2007GL029797.

- Wang, X., C. L. Heald, D. A. Ridley, J. P. Schwarz, J. R. Spackman, A. E. Perring, H. Coe, and D. Liu. 2014. Exploiting Simultaneous Observational Constraints on Mass and Absorption to Estimate the Global Direct Radiative Forcing of Black Carbon and Brown Carbon. *Atmos. Chem. Phys.* 14: 10989–10. doi.org/10.5194/acp-14-10989-2014.
- Wang, Y., P. L. Ma, J. Peng, R. Zhang, J. H. Jiang, R. C. Easter, and Y. L. Yung. 2018. Constraining Aging Processes of Black Carbon in the Community Atmosphere Model Using Environmental Chamber Measurements. *Journal of Advances in Modeling Earth Systems* 10 (10): 2514–26. doi.org/10.1029/2018MS001387.
- Wiegand, J. R., L. D. Mathews, and G. D. Smith. 2014. A UV-Vis Photoacoustic Spectrophotometer. *Anal. Chem.* 86 (12): 6049–56. doi.org/10.1021/ac501196u.
- Wu, G. M., Z. Y. Cong, S. C. Kang, K. Kawamura, P. Q. Fu, Y. L. Zhang, X. Wan, S. P. Gao, and B. Liu. 2016. Brown Carbon in the Cryosphere: Current Knowledge and Perspective. *Advances in Climate Change Research* 7 (1–2): 82–89. doi.org/10.1016/j.accre.2016.06.002.
- Xie, M., X. Chen, M. D. Hays, M. Lewandowski, O. John, T. E. Kleindienst, and A. L. Holder. 2017. Light Absorption of Secondary Organic Aerosol: Composition and Contribution of Nitroaromatic Compounds. *Environ. Sci. Technol.* 51: 11607–11616. doi.org/10.1021/acs.est.7b03263.
- Xie, M., M. D. Hays, and A. L. Holder. 2017. Light-Absorbing Organic Carbon from Prescribed and Laboratory Biomass Burning and Gasoline Vehicle Emissions. *Scientific Reports* 7 (1): 1–9. doi.org/10.1038/s41598-017-06981-8.
- Zhang, X., Y. H. Lin, J. D. Surratt, and R. J. Weber. 2013. Sources, Composition and Absorption Angström Exponent of Light-Absorbing Organic Components in Aerosol Extracts from the Los Angeles Basin. *Environ. Sci. Technol.* 47 (8): 3685–93. doi.org/10.1021/es305047b.